mode conversion, because both 15 GHz and 9 GHz conditions cannot be satisfied at the same time. The final design of the mode converter is shown in Figure 2. Three dielectric rods are located at the center of the waveguide. Two of these have $r = 0.515$ mm and the remainder have a half cross-section radius of 0.36 mm in order to decrease electromagnetic reflection. Nine dielectric rods are placed from the center of the waveguide to near the sidewall with increasing radius of the rods r and with constant $a = 9.54$ mm. Table 1 shows the relation between the distance d and radius r. The S parameters between the input port (Port 1) and output port (Port 2) are calculated using the HFSS software by Ansoft and the results are shown as solid lines in Figures 4(a) and 4(b). The electromagnetic waves pass through as the TE_{10} mode for 7–11.2 GHz and are converted to the TE_{20} mode for 14.1–16.1 GHz under a condition of over 95% efficiency. However, as the TE_{20} mode is not sufficiently small under −15 dB, optimization of the design is necessary for reduction of reflections. Although reflection as TE_{20} is not small at high frequency, if a coaxial waveguide converter is used for the introduction of electromagnetic waves to a waveguide, odd mode may not have a strong influence on even symmetry structure.

3. SIMPLE FABRICATION METHOD

For the fabrication of a mode converter, such as, the Type A illustrated in Figure 5(a), it is necessary to locate the dielectric rods in the waveguide without a gap at top and bottom. Such a structure may be difficult to fabricate. As a solution, holes with diameter 0.2 mm larger than the rods were fabricated at the top of the waveguide and the dielectric rods were inserted [Type B, Fig. 5(b)]. The S parameters were calculated using the HFSS software and the results are shown as dotted lines in Figures 4(a) and 4(b). The results for these different structural conditions (solid lines and dotted lines) are almost same.

4. CONCLUSIONS

We have previously reported that single-mode propagation is available for a metallic waveguide with dielectric rods arrayed at the center of a waveguide using the TE_{10} mode and the TE_{20} mode. However, a TE_{20}-like mode, which is propagated in the second band, is an odd mode, and generation is not easy. In this investigation, a mode converter is proposed, which passes through the TE_{10} mode for the low frequency range and converts TE_{10} to the TE_{20} mode for the high frequency range by small variation in the group velocity. It was shown that the electromagnetic waves pass through as the TE_{10} mode for 7–11.2 GHz and are converted to the TE_{20} mode for 14.1–16.1 GHz under a condition of over 95% efficiency.

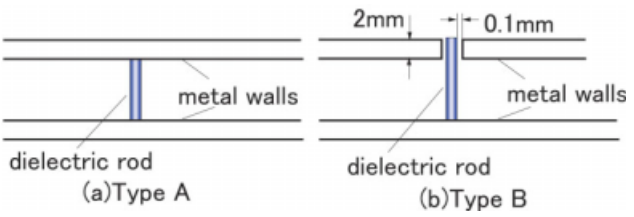

Figure 5 (a) Dielectric rod located in a waveguide without gaps at top and bottom. (b) Dielectric rod inserted in a hole made at the top of the waveguide with a diameter 0.2 mm larger than the diameter of the rod. [Color figure can be viewed in the online issue, which is available at www.interscience.wiley.com]

REFERENCES

1. S.B. Cohn, Properties of ridge wave guide, Proc IRE 35 (1947), 783–788.
2. Y. Kokubo, Wide band metallic waveguide with in-line dielectric rods, IEICE Trans Electron J90-C (2007), 642–643.
3. Y. Kokubo and T. Kawai, 90-degree H-plane bent waveguide using dielectric rods, Microwave Opt Technol Lett 51 (2009).
4. H. Benisty, Modal analysis of optical guides with two-dimensional photonic band-gap boundaries, J Appl Phys 79 (1996), 7483–7492.
5. M. Boroditsky, R. Coccioli, and E. Yablonovitch, Analysis of photonic crystals for light emitting diodes using the finite difference time domain technique, Proc SPIE 3283 (1998), 184–190.
6. Y. Kokubo and T. Kawai, Wide band metallic waveguide with asymmetric in-line dielectric rods, IEICE Trans Electron E-91-C (2008), 1966–1968.

VERY SMALL SIZE PRINTED MONOPOLE WITH EMBEDDED CHIP INDUCTOR FOR 2.4/5.2/5.8 GHz WLAN LAPTOP COMPUTER ANTENNA

Ting-Wei Kang and Kin-Lu Wong
Department of Electrical Engineering, National Sun Yat-Sen University, Kaohsiung 80424, Taiwan; Corresponding author: kangtw@ema.ee.nsysu.edu.tw

Received 5 April 2009

ABSTRACT: *A very small size planar two-strip monopole printed on a thin (0.4 mm) FR4 substrate for 2.4/5.2/5.8 GHz triple-band WLAN operation in the laptop computer is presented. With the aid of an embedded chip inductor of 5.6 nH in the longer strip of the printed monopole, a much reduced strip length for obtaining the resonant mode at about 2.4 GHz is obtained, thereby leading to a much reduced size of the antenna for the desired WLAN operation. When the antenna is mounted along the top edge of the display ground, it shows a height of 9 mm and a length of 6 mm only, which is about the smallest among the triple-band WLAN laptop computer antennas that have been reported. Details of the proposed antenna are described. Results of the fabricated prototype, including the user's hand effects on the antenna performances, are presented.* © 2009 Wiley Periodicals, Inc. Microwave Opt Technol Lett 52: 171–177, 2010; Published online in Wiley InterScience (www.interscience.wiley.com). DOI 10.1002/mop.24843

Key words: *mobile antennas; internal laptop computer antennas; printed monopoles; WLAN antennas; multiband antennas*

1. INTRODUCTION

In the modern laptop computers, decreasing thickness and size of the embedded internal antennas are demanded. This is mainly owing to the increasing internal antennas for various communication systems required therein and the trend for the thinner profile of the laptop computers. To meet the requirement, planar printed antennas are found to be attractive, and some promising designs for laptop computer applications have been reported recently [1–5]. With the planar printed structure, the recently reported promising laptop computer antennas capable of providing 2.4/5.2/5.8 GHz triple-band WLAN (wireless local area network) operation mainly use the coupled-fed PIFA (planar inverted-F antenna) or monopole elements [1–4]. The occupied size of these printed WLAN antennas has been reduced to be as small as 7×9 mm^2 (with a 1.6-mm thick FR4 substrate) [2]. That is, with an antenna height of 9 mm, which is less than that (about 10 mm) of the internal WWAN (wireless wide area

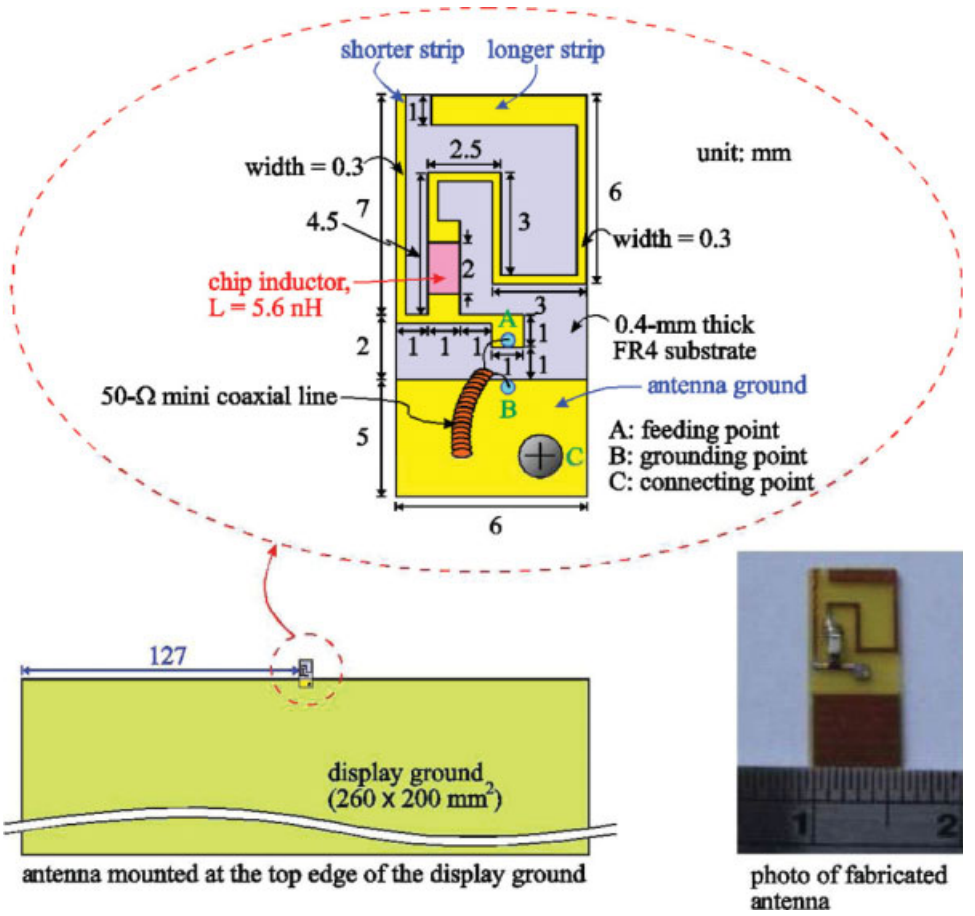

Figure 1 Geometry of the proposed printed monopole antenna embedded with a chip inductor for 2.4/5.2/5.8 GHz triple-band WLAN operation in the laptop computer. [Color figure can be viewed in the online issue, which is available at www.interscience.wiley.com]

network) laptop computer antennas [6–9] and is suitable for practical applications, the occupied length of the internal WLAN antenna along the top edge of the display ground (see Fig. 1) is 7 mm only. Such a small length is very attractive for laptop computer applications.

In this article, we present another promising uniplanar monopole antenna with a very small size of 6×9 mm^2 printed on a thin (0.4 mm only) FR4 substrate for covering 2.4 GHz (2400–2484 MHz) and 5.2/5.8 GHz (5150–5350/5725–5875 MHz) WLAN operation. Note that the antenna size of 6×9 mm^2 is smaller than that (7×9 mm^2) in [2], which uses a thick (1.6 mm) FR4 substrate. The proposed antenna is a simple two-strip monopole, and the much reduced size of the antenna is achieved by embedding a chip inductor in its longer strip of the printed monopole. The embedded chip inductor contributes additional inductance to compensate for the increased capacitance resulting from the decreased length of the radiating strip [10–12]. Details of the proposed printed monopole antenna are described, and results of the fabricated prototype are presented and discussed.

In addition, effects of the user's hand on the performances of the proposed antenna are studied for the case of the laptop computer equipped with the touch panel or touch display [13], which is expected to become popular for future laptop computers. In this case, as the user's hand is considered as a very lossy material [14–21], its effects on the radiation efficiency and radiation patterns of the proposed antenna will be interesting and also important for practical applications. Results obtained from the simulation model with the phantom hand provided by SPEAG SEMCAD [22] are analyzed.

2. PROPOSED MONOPOLE FOR TRIPLE-BAND WLAN OPERATION

Figure 1 shows the geometry of the proposed printed monopole antenna embedded with a chip inductor for 2.4/5.2/5.8 GHz triple-band WLAN operation in the laptop computer. The photo of the fabricated antenna printed on a 0.4-mm thick FR4 substrate of relative permittivity 4.4 in the experiment is also given in the figure. Note that when mounted along the top edge of the display ground of length 260 mm and width 200 mm (the antenna ground electrically connected to the display ground at point C), the antenna shows a height of 9 mm and a small length of 6 mm only. In the study, the antenna is mounted at the center of the top edge of the display ground. For testing the antenna, a 50-Ω mini coaxial line with its central conductor and outer grounding sheath connected to point A and point B (separated by a gap of 1 mm) is used in the experiment.

The radiating portion of the antenna is a simple two-strip monopole. The shorter strip has a length of about 11 mm, which is about 0.2 wavelength at about 5.5 GHz and can easily generate a wide resonant mode to cover WLAN operation in the 5.2/5.8 GHz bands. The longer strip is embedded with a chip inductor of 5.6 nH and has a total length of about 26 mm, which is about 0.2 wavelength at about 2.4 GHz. Owing to the embedded chip inductor, the resonant mode contributed by the longer strip can be effectively shifted to lower frequencies by about 1 GHz,

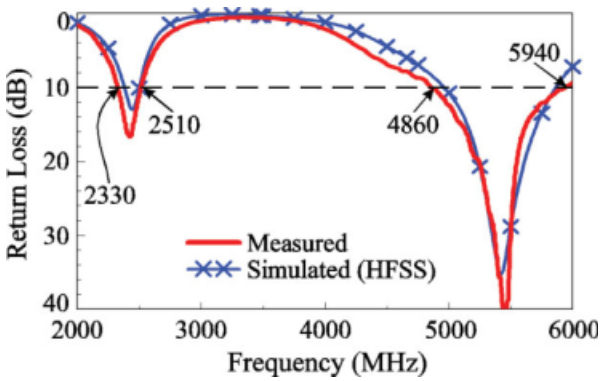

Figure 2 Measured and simulated return loss for the proposed antenna. [Color figure can be viewed in the online issue, which is available at www.interscience.wiley.com]

from at about 3.4–2.4 GHz (results shown in Fig. 3 in Section 3). Note that the embedded chip inductor is effective in decreasing the resonant frequency of the antenna's lower band, although the longer strip is meandered to achieve a much smaller size of the antenna and the meandering usually results in a decrease in the effective resonant length for a fixed physical strip length, owing to the coupling between adjacent meandered sections in the strip. With the proposed design, a wide resonant mode contributed by the longer strip for covering WLAN operation in the 2.4 GHz band is obtained. Hence, with the shorter strip and the chip-inductor-embedded longer strip, two wide bands can be generated for the antenna to cover 2.4 GHz and 5.2/5.8 GHz WLAN operation. The proposed antenna was fabricated and tested, and the results are presented in the next section.

3. RESULTS AND DISCUSSION

The measured data of the fabricated prototype with the parameters given in Figure 1 are presented in Figure 2. The simulated

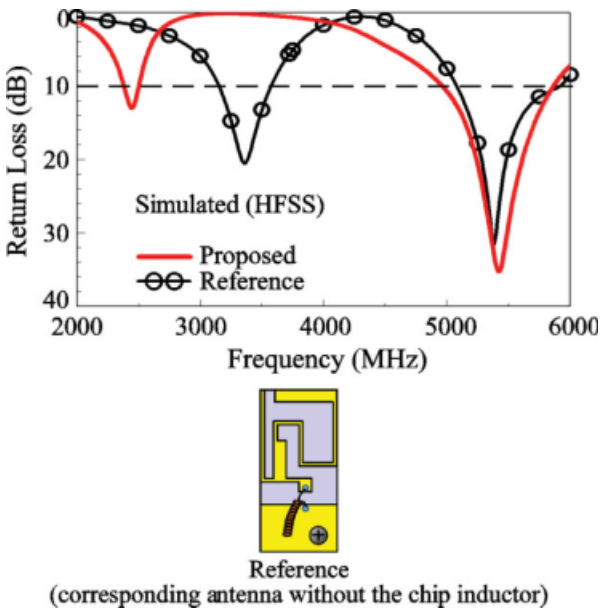

Figure 3 Simulated return loss for the proposed antenna and the reference antenna (the corresponding design without the chip inductor). [Color figure can be viewed in the online issue, which is available at www.interscience.wiley.com]

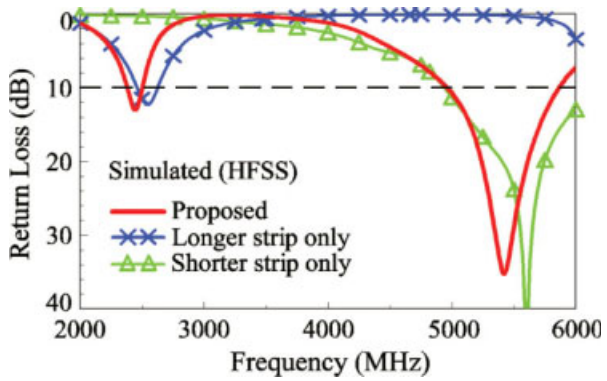

Figure 4 Simulated return loss for the proposed antenna, the case with the longer strip only, and the case with the shorter strip only. [Color figure can be viewed in the online issue, which is available at www.interscience.wiley.com]

results obtained using the Ansoft HFSS (high frequency structure simulator) [23] are also shown, and good agreement between the measured data and simulated results is obtained. From the results, two operating bands at about 2.4 and 5.5 GHz are generated, allowing the antenna to easily cover 2.4/5.2/5.5 GHz WLAN operation.

Figure 3 shows the simulated return loss for the proposed antenna and the reference antenna (the proposed antenna without the chip inductor as seen in the inset of the figure). It is clearly seen that, owing to the embedded chip inductor, the antenna's lower band is shifted to lower frequencies, from about 3.4–2.4 GHz as stated in Section 2, to cover the 2.4 GHz band for WLAN operation. For the antenna's upper band, relatively small effects on the obtained bandwidth are seen.

Effects of the two radiating strips of the proposed antenna are analyzed in Figure 4. Results of the simulated return loss for the proposed antenna, the case with the longer strip only, and the case with the shorter strip only are presented. It is clear that the antenna's lower and upper bands are contributed by the longer and shorter strips, respectively. Figure 5 shows the effects of varying the inductance of the embedded chip inductor on the antenna performances. Results for the inductance L of the embedded chip inductor varied from 4.7 to 6.8 nH are presented. Results indicate that the lower band is shifted to lower frequencies with increasing inductance L. This behavior is reasonable, since a larger inductance can compensate for the larger

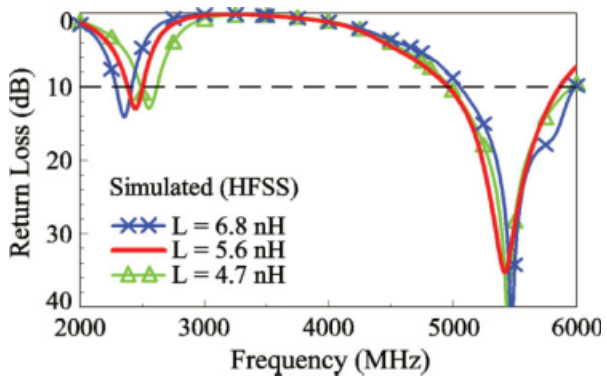

Figure 5 Simulated return loss of the proposed antenna as a function of the inductance L of the embedded chip inductor. [Color figure can be viewed in the online issue, which is available at www.interscience.wiley.com]

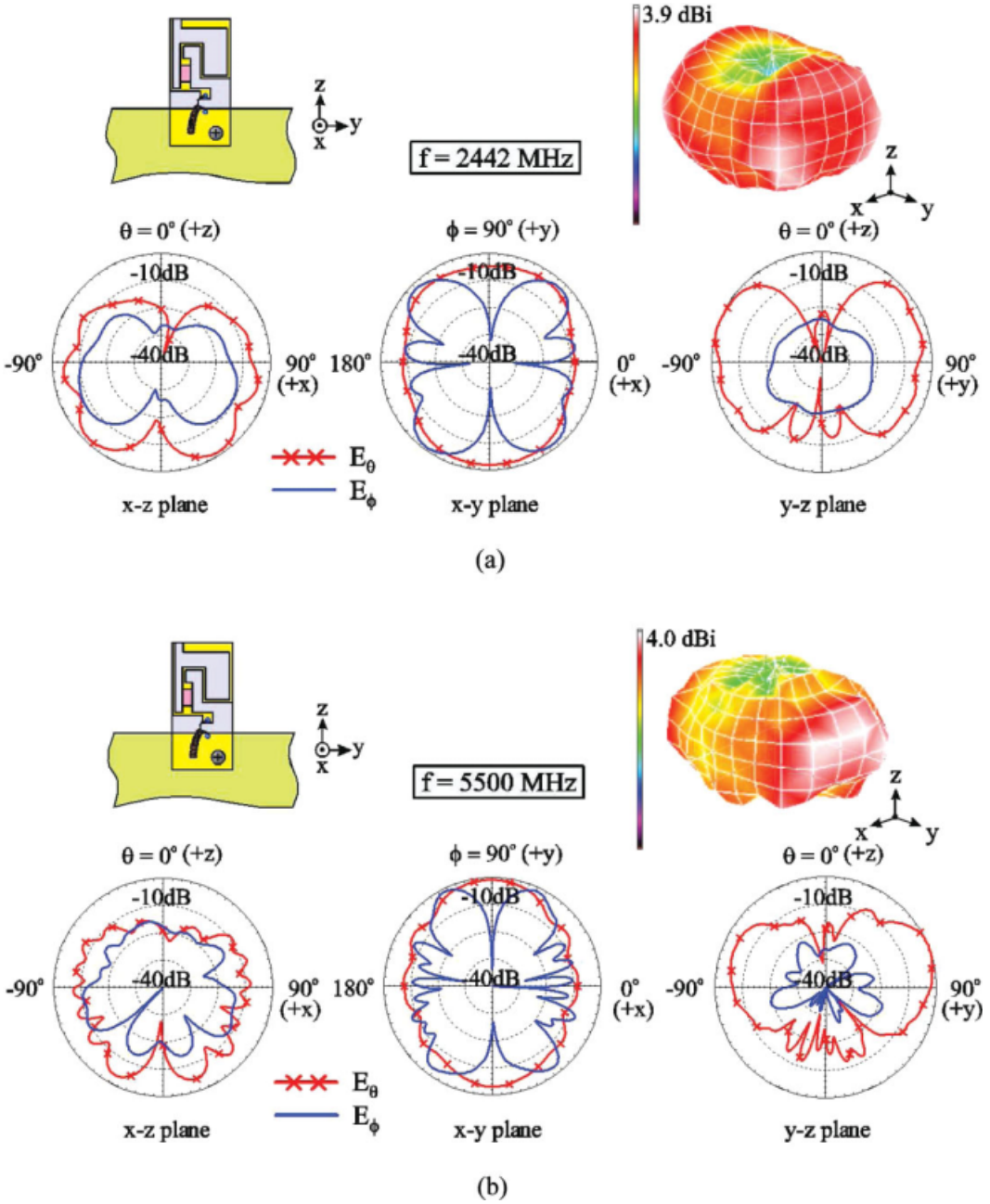

Figure 6 Measured 2D and 3D radiation patterns at (a) 2442 MHz and (b) 5500 MHz for the proposed antenna. [Color figure can be viewed in the online issue, which is available at www.interscience.wiley.com]

capacitance resulting from the longer strip with a smaller length [10–12]. As for the upper band, again, the obtained bandwidths are generally about the same.

Figure 6 plots the measured two-dimensional (2D) and three-dimensional (3D) radiation patterns at 2442 and 5500 MHz for the fabricated prototype. Monopole-like radiation patterns at the two frequencies are obtained, and omnidirectional total-power radiation in the *x-y* plane is generally seen, which is advantageous for practical applications. Figure 7 shows the measured antenna gain and radiation efficiency for the fabricated prototype. Over the 2.4 GHz band shown in Figure 7(a), the radiation efficiency is about 62–80%, and the antenna gain is varied from 2.8 to 3.9 dBi. For the 5.2/5.8 GHz bands shown in Figure 7(b), the radiation efficiency is about 60–74%, while the antenna gain is about 3.6–4.3 dBi. Results indicate that good radiation characteristics are obtained for the proposed antenna.

The measured average antenna gain in the azimuthal plane of the proposed antenna is also studied, which is demanded to be better than the specification [2] given in Table 1 for practical applications. The average antenna gain in the azimuthal plane is defined as the average of the antenna gain over all of the ϕ angles. This specification is imposed such that there will be no large dips or nulls in the antenna's radiation patterns in the azimuthal plane to ensure good coverage in all directions of the azimuthal plane of the laptop computer. The measured results of the average antenna gain for the proposed antenna are presented in Table 1. Results for the condition including the power loss of the long mini coaxial line (can be as long as about 70 cm)

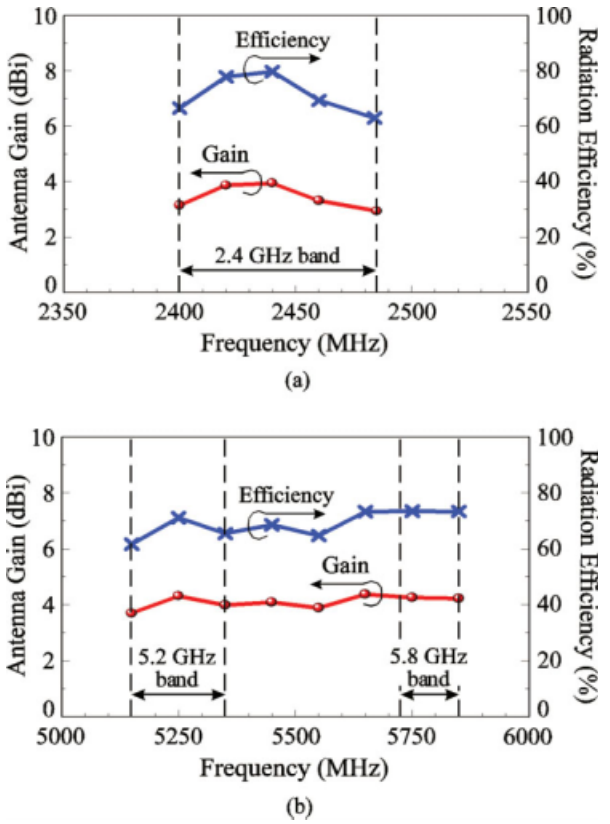

Figure 7 Measured antenna gain and radiation efficiency for the proposed antenna. (a) The 2.4 GHz band. (b) The 5.2/5.8 GHz bands. [Color figure can be viewed in the online issue, which is available at www.interscience.wiley.com]

connected to the internal antenna in the laptop computer are also given in the table. The power loss of the 70-cm long coaxial line is estimated to be −2 dB for frequencies over the 2.4 GHz band and −4 dB over the 5.2/5.8 GHz bands [2]. The obtained results indicate that the average antenna gain of the proposed antenna meets the specification for practical applications.

Effects of the user's hand in the proximity of the proposed antenna are also studied. Figure 8 shows the simulation model

TABLE 1 Measured Average Antenna Gain in the Azimuthal Plane of the Proposed Antenna

Average Antenna Gain (dBi)		Proposed Antenna (dBi)	Proposed Antenna with 70-cm Coaxial Line Loss (dBi)	Specification (dBi)
2.4 GHz band	2400 MHz	0.3	−1.7	−4.0
	2442 MHz	0.3	−1.7	−4.0
	2484 MHz	0.1	−1.9	−4.0
5.2/5.8 GHz bands	5150 MHz	1.3	−2.7	−5.0
	5350 MHz	1.3	−2.7	−5.0
	5500 MHz	1.3	−2.7	−5.0
	5725 MHz	1.3	−2.7	−5.0
	5875 MHz	1.1	−2.9	−5.0

The specification is the minimum average antenna gain required for practical applications of the internal WLAN antenna in the laptop computers [2].

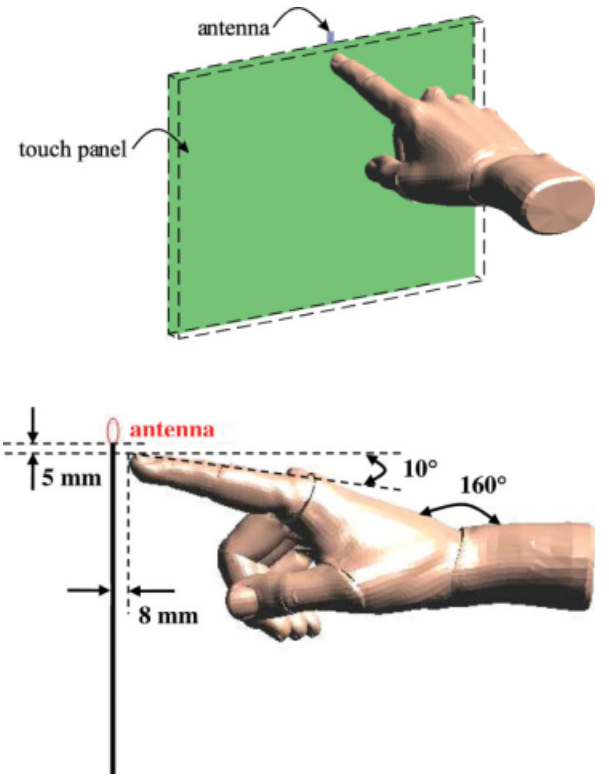

Figure 8 Simulation model for the proposed antenna with the phantom hand provided by SEMCAD-X [22]. [Color figure can be viewed in the online issue, which is available at www.interscience.wiley.com]

for the proposed antenna with the phantom hand provided by SEMCAD-X [22]. The case of the user's hand pointing at the top edge of the touch panel (assume to be 8 mm in thickness) and just below the proposed antenna is studied; the user's hand at this position is expected to have the strongest effects on the performances of the antenna. Figure 9 shows the simulated return loss for the proposed antenna with and without the phantom hand. It is interesting to note that the impedance matching for frequencies over the antenna's lower and upper bands is almost not affected by the phantom hand in the close proximity. However, from the simulated 3D radiation patterns at 2442 and 5500 MHz for the proposed antenna with and without the phantom hand shown in Figure 10, some effects of the user's hand on the radiation patterns are seen. There are some distortions in

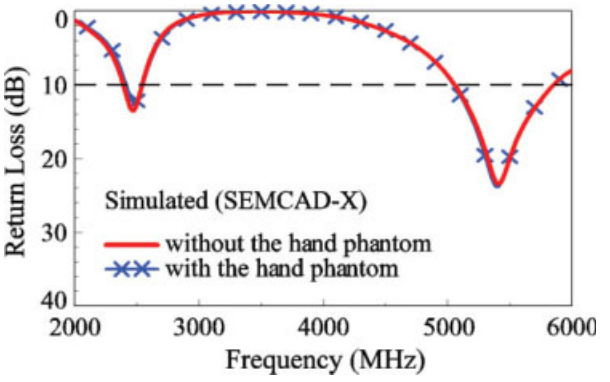

Figure 9 Simulated return loss for the proposed antenna with and without the phantom hand. [Color figure can be viewed in the online issue, which is available at www.interscience.wiley.com]

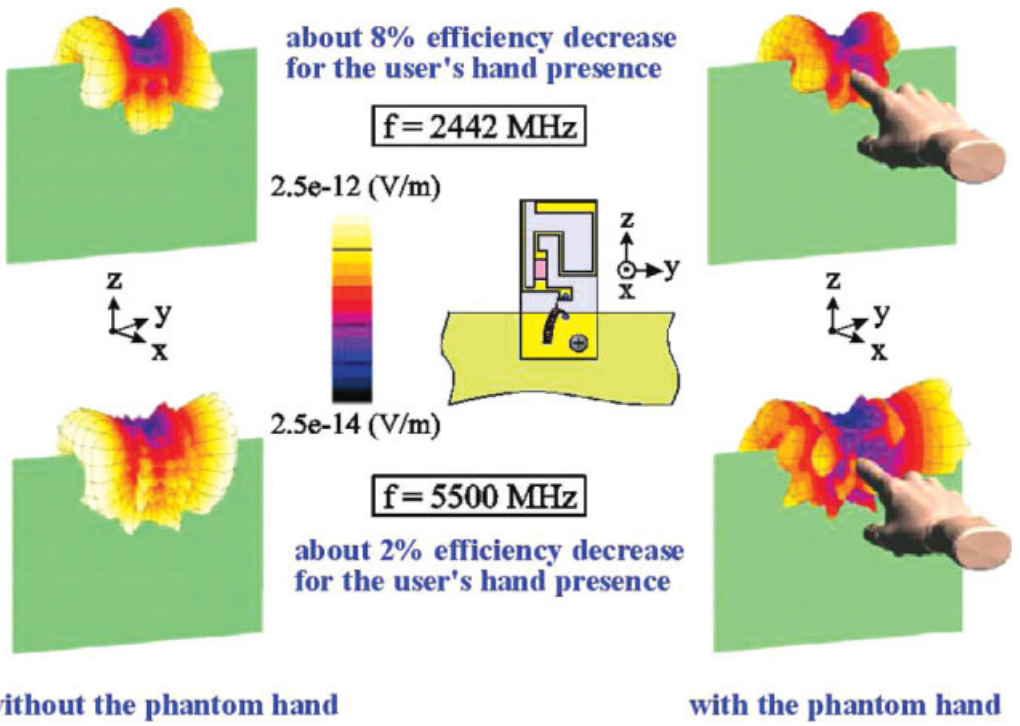

Figure 10 Simulated 3D radiation patterns at 2442 MHz and 5500 MHz for the proposed antenna with and without the phantom hand. [Color figure can be viewed in the online issue, which is available at www.interscience.wiley.com]

the radiation patterns observed owing to the presence of the user's hand, especially at 5500 MHz. For the radiation efficiency, a decrease of about 8% is seen at 2442 MHz, while that at 5500 MHz is about 2% only.

4. CONCLUSIONS

A printed monopole comprising a simple shorter strip and a chip-inductor-embedded longer strip, both together occupying a very small size of 6×9 mm^2, has been proposed for covering 2.4/5.2/5.8 GHz triple-band WLAN operation in the laptop computer. The embedded chip inductor (5.6 nH) effectively decreases the antenna's lower mode by about 1 GHz (from about 3.4–2.4 GHz), thus resulting in a much reduced size of the antenna. Good radiation characteristics for frequencies over the antenna's lower and upper bands have been obtained. Effects of the user's hand in the close proximity of the proposed antenna have also been analyzed. Results showed that the presence of the user's hand can cause large distortions in the antenna's radiation patterns and decrease the antenna's radiation efficiency by about 8% at 2442 MHz and about 2% at 5500 MHz. That is, effects of the user's hand on the antenna performances cannot be ignored for the internal WLAN laptop computer antennas.

REFERENCES

1. J. Yeo, Y.J. Lee, and R. Mittra, A novel dual-band WLAN antenna for notebook platforms, IEEE Antennas Propag Soc Int Symp Dig 2, Monterey, CA, USA, 2004, pp. 1439–1442.
2. S.J. Liao, K.L. Wong, and L.C. Chou, Small-size uniplanar coupled-fed PIFA for 2.4/5.2/5.8 GHz WLAN operation in the laptop computer, Microwave Opt Technol Lett 51 (2009), 1023–1028.
3. K.L. Wong and W.J. Chen, Small-size microstrip-coupled printed PIFA for 2.4/5.2/5.8 GHz WLAN operation in the laptop computer, Microwave Opt Technol Lett 51 (2009).
4. L.C. Chou and K.L. Wong, Uni-planar dual-band monopole antenna for 2.4/5 GHz WLAN operation in the laptop computer, IEEE Trans Antennas Propagat 55 (2007), 3739–3741.
5. K.L. Wong and F.H. Chu, Internal planar WWAN laptop computer antenna using monopole slot elements, Microwave Opt Technol Lett 51 (2009), 1274–1279.
6. C.H. Chang and K.L. Wong, Internal coupled-fed shorted monopole antenna for GSM850/900/1800/1900/UMTS operation in the laptop computer, IEEE Trans Antennas Propag 56 (2008), 3600–3604.
7. C.H. Kuo, K.L. Wong, and F.S. Chang, Internal GSM/DCS dual-band open-loop antenna for laptop application, Microwave Opt Technol Lett 49 (2007), 680–684.
8. X. Wang, W. Chen, and Z. Feng, Multiband antenna with parasitic branches for laptop applications, Electron Lett 43 (2007), 1012–1013.
9. K.L. Wong and L.C. Chou, Internal cellular/WLAN combo antenna for laptop-computer applications, Microwave Opt Technol Lett 47 (2005), 402–406.
10. T.W. Kang and K.L. Wong, Chip-inductor-embedded small-size printed strip monopole for WWAN operation in the mobile phone, Microwave Opt Technol Lett 51 (2009), 966–971.
11. T.H. Chang and J.F. Kiang, Meshed antenna reduction by embedding inductors, IEEE Antennas Propagat Soc Int Symp and USNC/URSI Nat Radio Sci Meeting, Washington, DC, USA, 2005, Session 78.
12. J. Thaysen and K.B. Jakobsen, A size reduction technique for mobile phone PIFA antennas using lumped inductors, Microwave J 48 (2005), 114–126.
13. Wikipedia, the Free Encyclopedia. Available at: http://en.wikipedia.org/wiki/Touchscreen.
14. C.M. Su, C.H. Wu, K.L. Wong, S.H. Yeh and C.L. Tang, User's hand effects on EMC internal GSM/DCS dual-band mobile phone antenna, Microwave Opt Technol Lett 48 (2006), 1563–1569.
15. C.H. Wu, K.L. Wong, C.I. Lin, C.M. Su, S.H. Yeh, and C.L. Tang, Simplified hand model including the user's forearm for the study of internal GSM/DCS mobile phone antenna, Microwave Opt Technol Lett 48 (2006), 2202–2205.

16. C.I. Lin and K.L. Wong, Internal meandered loop antenna for GSM/DCS/PCS multiband operation in a mobile phone with the user's hand, Microwave Opt Technol Lett 49 (2007), 759–765.
17. C.H. Wu, K.L. Wong, Y.C. Lin, and S.W. Su, Internal shorted monopole antenna for the watch-type wireless communication device for Bluetooth operation, Microwave Opt Technol Lett 49 (2007), 942–946.
18. C.I. Lin and K.L. Wong, Printed monopole slot antenna for internal multiband mobile phone antenna, IEEE Trans Antennas Propag 55 (2007), 3690–3697.
19. W.Y. Li, K.L. Wong, and J.S. Row, Study of the planar DTV antenna in the portable media player held by the user's hands, Microwave Opt Technol Lett 49 (2007), 1841–1844.
20. C.H. Wu and K.L. Wong, Internal shorted planar monopole antenna embedded with a resonant spiral slot for penta-band mobile phone application, Microwave Opt Technol Lett 50 (2008), 529–536.
21. C.T. Lee and K.L. Wong, Uniplanar coupled-fed printed PIFA for WWAN/WLAN operation in the mobile phone, Microwave Opt Technol Lett 51 (2009), 1250–1257.
22. SEMCAD, Schmid and Partner Engineering AG (SPEAG). Available at: http://www.semcad.com.
23. Ansoft Corporation HFSS. Available at: http://www.ansoft.com/products/hf/hfss/.

MICROWAVE SIGNAL GENERATION BASED ON TWO SINGLE-LONGITUDINAL-MODE ERBIUM-DOPED FIBER LASERS

Jian-Hua Luo,[1] Bo Liu,[1] Hao Zhang,[1] Shao-Lin Yan,[1] Xiu-Rong Ma,[2] and Cheng-Lai Jia[1]
[1] College of Information Technical Science, Key Laboratory of Opto-electronic Information Science and Technology, Ministry of Education, Nankai University, Tianjin 300071, China; Corresponding author: lubilin@mail.nankai.edu.cn
[2] School of Computer and Communication Engineering, Tianjin University of Technology, Tianjin 300384, China

Received 5 April 2009

ABSTRACT: *A simple microwave signal source is proposed by connecting two single-longitudinal-mode erbium-doped distributed Bragg reflector fiber lasers in series. For using same pump LD, mutual injection locking of two fiber lasers is achieved. The two single-longitudinal-mode lasers have 0.048 nm wavelength difference. By beating the two wavelengths at a photodetector, stable microwave signal at 6.17 GHz is achieved at room temperature.* © 2009 Wiley Periodicals, Inc. Microwave Opt Technol Lett 52: 177–179, 2010; Published online in Wiley InterScience (www.interscience.wiley.com). DOI 10.1002/mop.24840

Key words: *microwave signal; distributed Bragg reflector; single-longitudinal-mode; mutual injection locking*

1. INTRODUCTION

Recently, single-longitudinal-mode fiber laser attracted widespread attention for its application in a variety of fields including spectroscopy, resonant cavity frequency doubling, coherent optics, and communication. Lots of researches were reported at home and abroad [1, 2]. Based on a complex structured (equivalent) phase-shifted FBG, dual-wavelength SLM lasing and microwave signal (based on the two lasing wavelengths) can be achieved [3, 4]. Some recent works [4, 5] have shown that stable dual-wavelength lasing at room temperature based on an erbium-doped fiber (homogeneous gain medium) is possible. However, it often requires some complex-structured phase-shifted FBG (with an ultra-narrow transmission band), which is difficult to fabricate and requires a very good writing system.

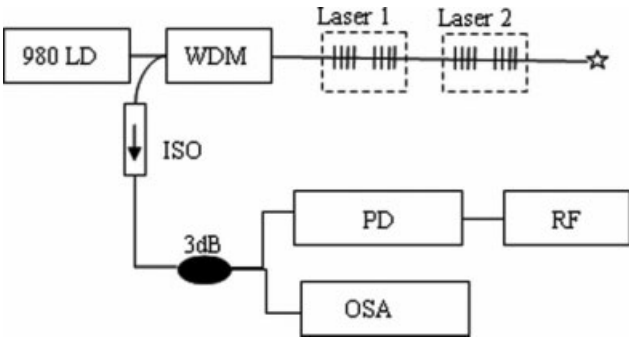

Figure 1 The schematic configuration of the proposed microwave signal source

Fiber lasers are usually of multi-longitudinal-mode (MLM) operation with mode hopping due to a long cavity and very narrow longitudinal mode spacing. A DBR fiber laser with a very short linear cavity can achieve SLM lasing [6]. Chen et al. [7] reported a dual-wavelength single-longitudinal-mode erbium-doped fiber laser based on fiber Bragg grating pair which used FBG pair instead of a superstructured phase-shifted FBG. In this article, we report a microwave signal generation based on two single-longitudinal-mode erbium-doped fiber lasers which have 0.048 nm wavelength difference. By beating the two wavelengths at a photodetector, stable microwave signal at 6.17 GHz is achieved at room temperature.

2. EXPERIMENTAL SETUP AND RESULTS

The schematic configuration of the proposed microwave signal source is shown in Figure 1. Two DBR fiber lasers with very short linear cavity are used as SLM lasing. Laser 1 incorporates two 1542.32 nm FBGs as the resonator mirrors with a section of 15 mm EDF as the gain medium. One of the two gratings is 11-mm long and has a higher reflectivity of more than 99%; the other grating is 5.8-mm long with a lower reflectivity of around 90%. In Laser 2, two 1542.37 nm gratings are linked by 15 mm EDF. The length of one grating is 10-mm long with a higher reflectivity of more than 99%, while the other grating is 6-mm long with a lower reflectivity of around 90%.

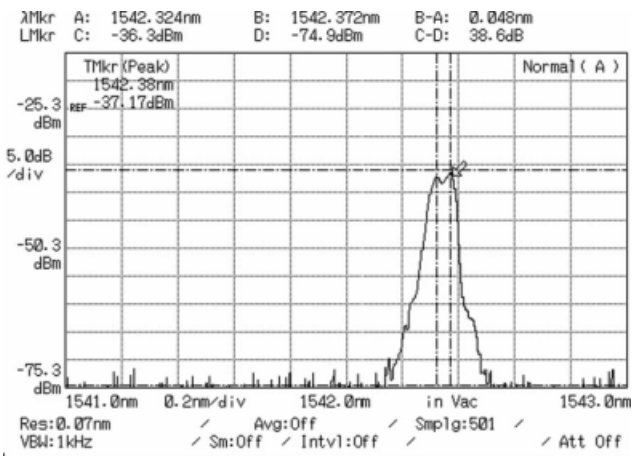

Figure 2 The optical spectrum of the two connecting lasers